Metadata of the chapter that will be visualized online

Chapter Title	Multispectral Optoacoustic Tomography of Brown Adipose Tissue	
Copyright Year	2018	
Copyright Holder	Springer International Publishing AG, part of Springer Nature	
Author	Family Name	**Karlas**
	Particle	
	Given Name	**Angelos**
	Suffix	
	Division	Biological Imaging
	Organization	Technical University Munich
	Address	Munich, Germany
	Organization	Institute for Biological and Medical Imaging (IBMI), Helmholtz Zentrum München
	Address	Neuherberg, Germany
Author	Family Name	**Reber**
	Particle	
	Given Name	**Josefine**
	Suffix	
	Division	Biological Imaging
	Organization	Technical University Munich
	Address	Munich, Germany
	Organization	Institute for Biological and Medical Imaging (IBMI), Helmholtz Zentrum München
	Address	Neuherberg, Germany
Author	Family Name	**Liapis**
	Particle	
	Given Name	**Evangelos**
	Suffix	
	Division	Biological Imaging
	Organization	Technical University Munich
	Address	Munich, Germany
	Organization	Institute for Biological and Medical Imaging (IBMI), Helmholtz Zentrum München
	Address	Neuherberg, Germany
Author	Family Name	**Paul-Yuan**
	Particle	
	Given Name	**Korbinian**
	Suffix	

	Division	Biological Imaging
	Organization	Technical University Munich
	Address	Munich, Germany
	Organization	Institute f🗨iological and Medical Imaging (IBMI), Helmholtz Zentrum München
	Address	Neuherberg, Germany
Corresponding Author	Family Name	**Ntziachristos**
	Particle	
	Given Name	**Vasilis**
	Suffix	
	Division	Biological Imaging
	Organization	Technical University Munich
	Address	Munich, Germany
	Organization	Institute f🗨iological and Medical Imaging (IBMI), Helmholtz Zentrum München
	Address	Neuherberg, Germany
	Email	v.ntziachristos@tum.de

Abstract	MSOT has revolutionized biomedical imaging because it allows anatomical, functional, and molecular imaging of deep tissues in vivo in an entirely noninvasive, label-free, and real-time manner. This imaging modality works by pulsing light onto tissue, triggering the production of acoustic waves, which can be collected and reconstructed to provide high-resolution images of features as deep as several centimeters below the body surface. Advances in hardware and software continue to bring MSOT closer to clinical translation. Most recently, a clinical handheld MSOT system has been used to image brown fat tissue (BAT) and its metabolic activity by directly resolving the spectral signatures of hemoglobin and lipids. This opens up new possibilities for studying BAT physiology and its role in metabolic disease without the need to inject animals or humans with contrast agents. In this chapter, we overview how MSOT works and how it has been implemented in preclinical and clinical contexts. We focus on our recent work using MSOT to image BAT in resting and activated states both in mice and humans.

Keywords (separated by '-')	■■■ 🗨

Multispectral Optoacoustic Tomography of Brown Adipose Tissue

1
2 AU1

Angelos Karlas, Josefine Reber, Evangelos Liapis,
Korbinian Paul-Yuan, and Vasilis Ntziachristos

3

4

Contents

5

Abstract

MSOT has revolutionized biomedical imaging because it allows anatomical,   13
functional, and molecular imaging of deep tissues in vivo in an entirely noninva-   14
sive, label-free, and real-time manner. This imaging modality works by pulsing   15
light onto tissue, triggering the production of acoustic waves, which can be   16
collected and reconstructed to provide high-resolution images of features as   17
deep as several centimeters below the body surface. Advances in hardware and   18
software continue to bring MSOT closer to clinical translation. Most recently, a   19
clinical handheld MSOT system has been used to image brown fat tissue (BAT)   20
and its metabolic activity by directly resolving the spectral signatures of hemo-   21
globin and lipids. This opens up new possibilities for studying BAT physiology   22
and its role in metabolic disease without the need to inject animals or humans   23
with contrast agents. In this chapter, we overview how MSOT works and how it   24

Angelos Karlas and Josefine Reber contributed equally to this work.   AU2

A. Karlas · J. Reber · E. Liapis · K. Paul-Yuan · V. Ntziachristos (✉)
Biological Imaging, Technical University Munich, Munich, Germany

Institute for Biological and Medical Imaging (IBMI), Helmholtz Zentrum München, Neuherberg,
Germany
e-mail: v.ntziachristos@tum.de

has been implemented in preclinical and clinical contexts. We focus on our recent work using MSOT to image BAT in resting and activated states both in mice and humans.

AU3

Purely optical imaging techniques such as optical microscopy, endoscopy, and optical coherence tomography rely on light-tissue interactions for high-contrast imaging in vivo and ex vivo (Weissleder and Pittet 2008). However, light scattering and absorption degrade image resolution with increasing depth and gradually attenuate the available light energy, limiting the effective imaging depth to a few hundred microns (Ntziachristos 2010). Non-optical techniques are usually used to image beyond these depths, including X-ray computed tomography (CT), magnetic resonance imaging (MRI), ultrasound (US), positron emission tomography (PET), and single-photon emission tomography (SPECT). These non-optical techniques present disadvantages that limit their use in the clinic, including the need for ionizing radiation (CT, PET, and SPECT) or for expensive, bulky equipment (MRI, PET, and SPECT).

AU4

Optoacoustics (OA) overcomes the depth limitations of optical imaging techniques because, as a hybrid technique, it generates an image based not only on light but also on acoustic waves. In OA, the tissue is illuminated with pulsed laser light, which is absorbed and causes minimal local heating, which leads in turn to thermoelastic expansion (Ntziachristos and Razansky 2010). This expansion generates acoustic waves, usually within the range of ultrasound, which travel out of the tissue and are detected by ultrasound transducers. The detected waves are then reconstructed into planar images. Since acoustic waves are scattered much less strongly than light as they travel through tissue, OA can image down to depths of ~2–5 cm, compared to a maximum of only ~1 mm for optical imaging techniques (Ntziachristos 2010). While OA cannot yet achieve the penetration depth of US, it offers superior, optical contrast (Ntziachristos and Razansky 2010) while retaining the usability of US imaging systems.

Of the various types of OA developed so far, multispectral optoacoustic tomography (MSOT) has made the greatest progress toward clinical translation (Dean-Ben et al. 2017). MSOT has already demonstrated its usefulness in several fields, including vascular medicine, breast oncology, thyroid imaging, muscle hemodynamics, and white adipose tissue (WAT) imaging (Karlas et al. 2017; Taruttis et al. 2016; Diot et al. 2015, 2017; Dima and Ntziachristos 2016; Buehler et al. 2017). Most recently, our group has shown that MSOT can image brown adipose tissue (BAT) and its metabolic activity in mice and humans without the need for injecting potentially toxic contrast agents. This opens up new possibilities for noninvasive, longitudinal investigation of BAT composition and physiology as well as their changes in disease (Reber et al. 2018).

1 The Multispectral Optoacoustic Tomography Principle

In MSOT, tissue is repeatedly excited with sequential pulses of near-infrared (NIR) laser light covering, for example, such wavelength ranges as 680–980 nm in 10-nm steps. The resulting ultrasound responses are captured using an array of usually 256 or 512 piezoelectric sensors. MSOT works in single-pulse-per-frame (SPPF) mode: each ultrafast laser pulse (duration of ∼10 ns) generates a broadband ultrasound response with energy in the frequency range of ∼0.5–7 MHz (Fig. 1). Custom-developed reconstruction methods are used to generate a tomographic image from the recorded ultrasound response to each single-wavelength pulse (Ntziachristos and Razansky 2010). Modern MSOT systems achieve frame rates of up to 50 Hz, allowing a complete series of single-wavelength frames covering all user-selected wavelengths (known as a "multispectral stack") to be recorded in less than a second. The varying intensity of each pixel along a multispectral stack gives the absorption spectrum of the tissue at that pixel position. In this way, MSOT adds the fifth dimension of spectrum to four-dimensional spatiotemporal imaging. Finally, the absorption spectrum at each pixel can be decomposed into known absorption spectra of biomedically relevant chromophores, such as hemoglobin, lipids, and water. This step allows the recorded absorption spectra to be translated into contributions from the various chromophores through a process known as "spectral unmixing." Such a process can reveal the distribution of light-absorbing molecules in living tissue with picomolar sensitivity (Ntziachristos and Razansky 2010; Diot et al. 2017).

2 Sources of Contrast in Multispectral Optoacoustic Tomography

Like purely optical imaging techniques, MSOT can image the contrast produced by externally administered agents, such as fluorescent dyes, nanoparticles, and photosensitizers, provided they absorb in the NIR region and have low quantum yield (Gujrati et al. 2017). Indocyanine green (ICG), already in clinical use for more than half a century, is the NIR dye most often used in OA (Philip et al. 1996). Nevertheless, the real advantage of MSOT over all other purely optical as well as non-optical imaging techniques is its ability to simultaneously detect several endogenous chromophores, including hemoglobin, melanin, lipids, and water, without the need for injecting external agents such as ICG. This equips MSOT with the ability to measure a broad range of physiological and pathophysiological processes such as tissue oxygenation, vascularization, and atherosclerosis (Weber et al. 2016).

MSOT can image and quantify various endogenous tissue chromophores through its ability to recognize the spectral signatures of each chromophore within acoustic signals collected over a range of wavelengths (Weissleder 2001). The most abundant intrinsic chromophore is hemoglobin, the iron-containing protein inside the red blood cells of all vertebrates that delivers oxygen throughout the body. When oxygen binds to the heme group of hemoglobin, the protein undergoes structural and electronic changes that alter its absorption spectrum. MSOT can detect these spectral changes, allowing the discrimination between oxy- and deoxyhemoglobin,
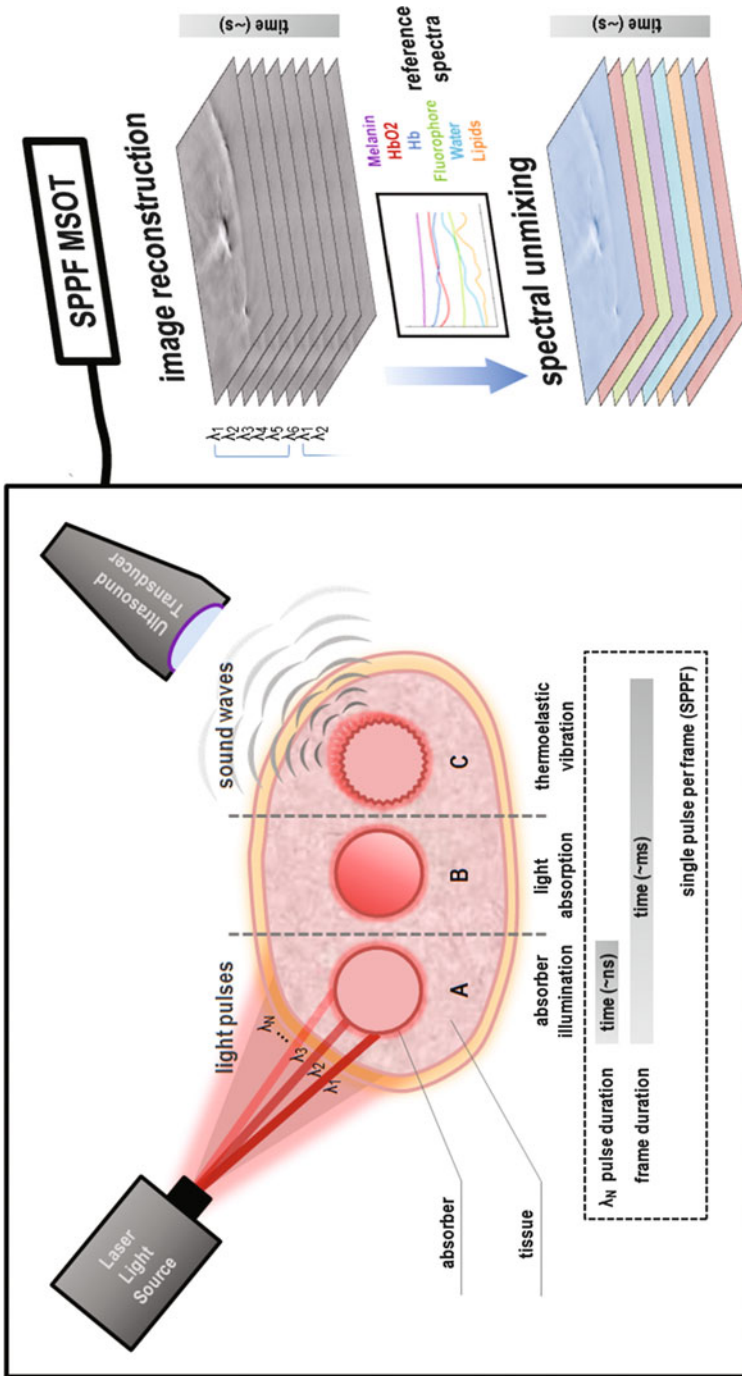
Fig. 1 The operating principle of MSOT. Light pulses with different NIR wavelengths ($\lambda_1, \lambda_2, \lambda_3 \ldots \lambda_N$) illuminate the tissue of interest, and chromophores within the tissue absorb the light, leading to transient local heating that triggers thermoelastic expansion. This expansion generates acoustic waves that propagate in all directions and are detected by an array of ultrasound detectors at the surface of the tissue. Multispectral stacks of single-wavelength tomographic images are produced using specific reconstruction methods. Decomposition of measured spectrum at each pixel across the N wavelengths in the stack (six in this example) into the known reference spectra of biological chromophores such as melanin and hemoglobin allows "unmixing" of the total image into images of different chromophores. HbO_2 oxygenated hemoglobin, Hb deoxygenated hemoglobin

measurement of their respective concentrations, calculation of total hemoglobin concentration [also known as total blood volume (TBV)], and estimation of blood oxygen saturation (sO$_2$) (Laufer et al. 2012). Since MSOT illuminates tissue with light covering a broad range of NIR wavelengths, it can detect a similarly broad range of endogenous chromophores. The natural skin pigment melanin absorbs strongly in the visible and near-infrared ranges. Lipids absorb strongly around 930 nm, while water absorbs strongly around 970 nm. The NIR optical window of 680–980 nm is particularly useful because hemoglobin and water absorb much less in this window than at other wavelengths, allowing more sensitive detection of other chromophores even down to depths of several centimeters. For example, MSOT at these wavelengths can assess intra- and peritumoral vascularity and fat and water content in breast tumors in patients, greatly expanding on the information extracted by US (Diot et al. 2017).

Genetically encoded chromophores expand the contrast agents that MSOT can image noninvasively in preclinical animal studies (Weber et al. 2016). Reporter genes encoding OA-compatible proteins can be expressed in specific tissues at specific points in the development, creating unique experimental opportunities. For example, green fluorescent protein (GFP) and its derivatives, which revolutionized anatomical and functional optical microscopy, can also be detected by MSOT (Razansky et al. 2009). However, none of the GFP variants described so far absorbs strongly in the NIR window of 680–980 nm (Razansky et al. 2009). Starting from phytochromes, which are photo-sensory receptors that absorb light when covalently bound to a linear tetra-pyrrole such as biliverdin, researchers have recently developed fluorescent proteins that absorb light in the NIR range (Shu et al. 2009). For example, near-infrared fluorescent protein (iRFP) has been used for single-wavelength OA tomography in vivo, where it showed an absorption maximum at ~690 nm and good photodynamic stability (Filonov et al. 2012).

Another strategy when using genetically encoded chromophores is to express enzymes that generate OA-compatible small molecules. The prokaryotic *lacZ* gene can be expressed in mammalian tissues to generate the enzyme β-galactosidase, which can hydrolyze exogenously added X-gal to produce an intensely blue product readily detectable by OA imaging in the visible range (Cai et al. 2012). Another example is expressing the genes to endogenously produce violacein, which shows good photobleaching resistance similar to that of X-gal (Jiang et al. 2015). The tyrosinase gene, which encodes the key enzyme in melanin biosynthesis, can be expressed in otherwise non-melanogenic cells (Jathoul et al. 2015). Expression of tyrosinase allows creation of MSOT contrast without the need to administer an exogenous precursor.

Despite this range of potential chromophores, most MSOT studies have focused on the strong contrast provided by hemoglobin. The technique can provide noninvasive, longitudinal assessment of slow pathological processes such as angiogenesis and hypermetabolism (Omar et al. 2015; Herzog et al. 2012) as well as tumor hypoxia/oxygenation (Tzoumas et al. 2016). It can also monitor fast (sub-second) processes such as neural activity that alter hemodynamics and so can be detected as changes in blood oxygen saturation and total hemoglobin concentration (Gottschalk et al. 2015). In the

next section, we discuss the recently demonstrated ability of MSOT to track several endogenous chromophores in vivo in order to characterize BAT and monitor its activation and changes related to disease.

## 3 Label-Free Brown Fat Tissue Imaging Using Multispectral Optoacoustic Tomography

Our group reasoned that MSOT should be able to differentiate BAT from WAT on the basis of their differences in hemoglobin, lipid, and water composition, which should translate to different spectral characteristics. If so, MSOT could turn out to be a powerful tool for studying BAT activation in a noninvasive, longitudinal manner. Our work suggests that, indeed, by measuring changes in local hemoglobin gradients over time, MSOT can quantify BAT activation in mice following pharmacological stimulation and BAT activation in humans following cold exposure (Fig. 2). Below we discuss, in turn, the preclinical and clinical evidence showing that MSOT can image BAT activation.

3.1 Preclinical Brown Fat Tissue Imaging Using Multispectral Optoacoustic Tomography

AU5

MSOT has been validated in mouse, fish, and other animal models of health and disease for being able to quantitatively analyze endogenous and exogenous chromophores (Razansky et al. 2007). High-quality MSOT imaging depends on homogeneous illumination and ultrasound detection around the sample. In state-of-the-art preclinical MSOT systems, ultrasound detectors cover approximately 270° (Fig. 2). The animal
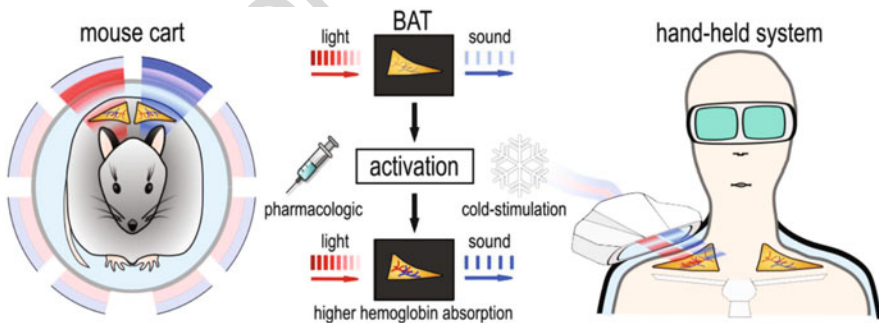
Fig. 2 Studying BAT activation in mice and humans using MSOT. The *image on the left* depicts the experimental setup for preclinical imaging, in which an anesthetized mouse is placed inside a cylindrical chamber within a larger measuring setup ("mouse cart"). Laser illumination of interscapular BAT deposits at various wavelengths generates acoustic waves, which are reconstructed into an image of BAT in the resting state. Then norepinephrine is injected intravenously to metabolically activate BAT, and the BAT deposits are imaged again. The *image on the right* depicts the experimental setup for clinical imaging of supraclavicular BAT activation with a handheld MSOT system. BAT was activated by cold stimulation using a cooling suit. Adapted with permission from Reber et al. (2018)

or excised tissue is placed in thin transparent foil (~100 μm) and then submerged in water at approximately 34°C. Typically, 45–60 min are needed to obtain a whole-body mouse scan in 300-μm steps along the *z*-axis.

3.1.1 Spectral Characterization of Mouse Adipose Tissue Ex Vivo

By designing and manufacturing appropriate biological imaging phantoms, the spectral signature of an excised tissue sample, such as BAT or WAT, can be accurately determined under tightly controlled experimental conditions. An ideal phantom should mimic the basic physical properties of living tissues such as optical absorption, scattering, and speed of sound. Phantoms can be used to analyze and optimize the imaging setup for subsequent in vivo or postmortem experiments. Excised tissues are typically examined within cylindrical phantoms with a diameter of ~2 cm and a composition of 1.3% (v/v) agar and 1.2% (v/v) fat emulsion. To investigate absorption spectra of mouse BAT and WAT, tissue samples were inserted into plastic tubes with a diameter of 3 mm, which were then inserted into the cylindrical phantom (Tzoumas et al. 2014). MSOT showed that OA signal intensity of BAT was more than twofold higher than that of WAT over the entire NIR range of 700–900 nm (Reber et al. 2018). This may be because the high density of iron-rich mitochondria makes BAT dark brown (Enerback 2009), which may explain its greater light absorption. BAT is also more highly vascularized than WAT, and the higher hemoglobin content may contribute to the greater absorption. MSOT has shown promising ability to detect lipid-based differences among BAT, WAT, and beige adipose tissue. Beige adipose tissue is thought to have a composition intermediate between that of BAT and WAT (Cedikova et al. 2016) and a function closer to that of BAT (Giralt and Villarroya 2013). The lipid spectrum of beige adipose tissue showed greater intensity than the lipid spectrum of WAT in the NIR range from 700 to 900 nm, yet the beige spectrum retained the characteristic WAT peak at 930 nm.

3.1.2 Imaging Mouse Adipose Tissue In Vivo

MSOT can track the contrast of hemoglobin to analyze tissue pathophysiology hallmarks (Tzoumas and Ntziachristos 2017), and the same contrast can allow tracking of BAT activation. BAT activation is followed by a substantial increase in blood flow (Ernande et al. 2016). MSOT can image interscapular BAT (iBAT), including the underlying Sulzer vein (SV), which provides the main venous drainage (Fig. 3a, b) (Reber et al. 2018). Spectral unmixing allows quantification of oxy- and deoxyhemoglobin content throughout iBAT and surrounding tissues, first in the resting state (Fig. 3d, g) and then following metabolic activation with norepinephrine (Fig. 3c, e, h), which increases BAT perfusion and induces BAT thermogenesis via consumption of glucose and lipid (Cypess et al. 2015). In our mouse studies, we found that norepinephrine altered hemoglobin levels only in the iBAT, not in surrounding muscle or other soft tissues (Fig. 3f, i). These results suggest that MSOT can serve as a powerful method for characterizing iBAT activation in mice and that the extent of iBAT vascularization can be quantified based on hemoglobin contrast.
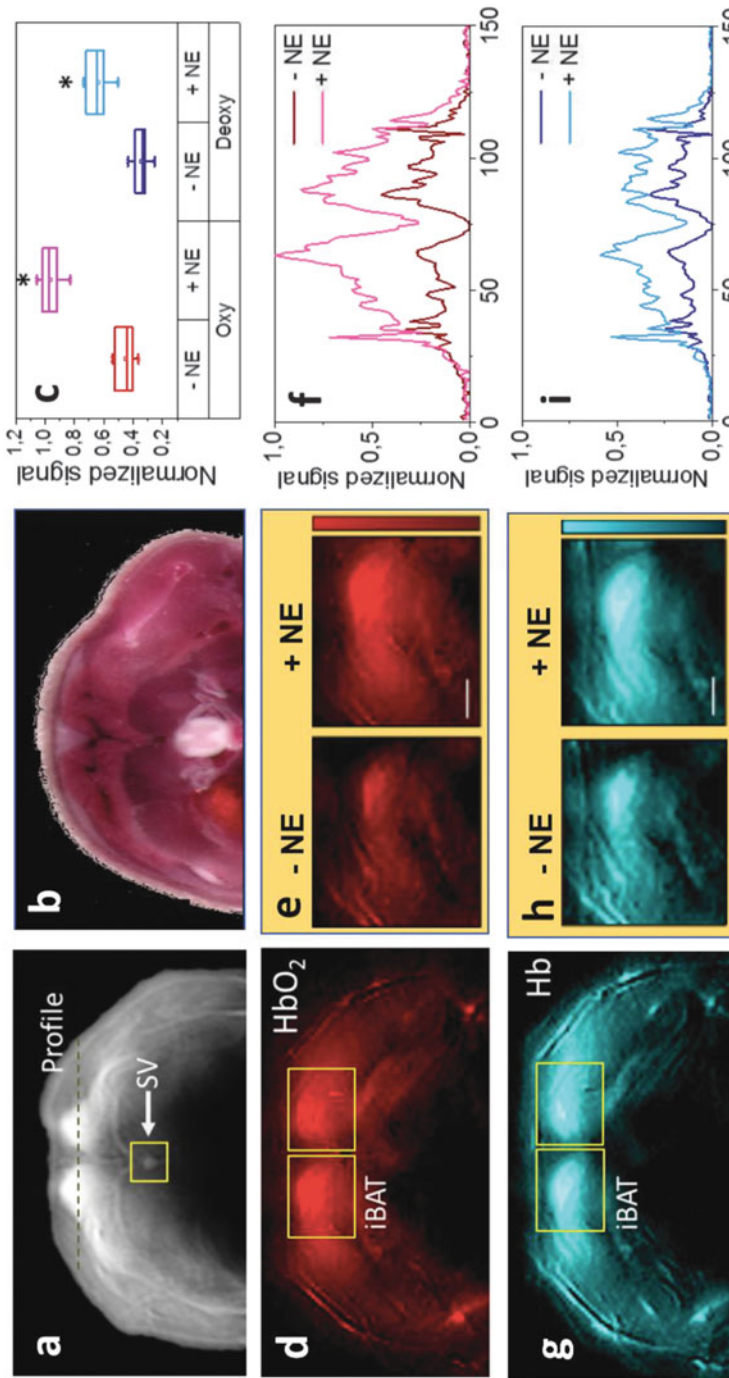
Fig. 3 In vivo imaging of interscapular BAT activation in mice using MSOT. (**a**) Reconstructed MSOT image (800 nm) showing interscapular BAT (iBAT) and the Sulzer vein (SV; yellow square). The black dashed line indicates the horizontal intensity profiles shown in panels (**f**) and (**i**). (**b**) Color image of a transverse cryoslice of the neck area, showing iBAT. (**c**) Boxplot of normalized signal intensities of oxyhemoglobin (HbO$_2$) and deoxyhemoglobin (Hb) in iBAT before and after activation with norepinephrine (NE). (**d–f**) Relative HbO$_2$ intensity in iBAT lobes before and after activation with NE. The close-up view in panel (**e**) shows the right lobe. The corresponding horizontal intensity profile is shown in panel (**f**). (**g–i**) Relative Hb intensity in iBAT lobes before and after activation with NE. The close-up view in panel (**h**) shows the right lobe. The corresponding horizontal intensity profile is shown in panel (**i**). Reproduced with permission from Reber et al. (Reber et al. 2018)

3.2 Clinical Brown Fat Tissue Imaging Using Multispectral Optoacoustic Tomography

One of the factors driving the application of MSOT to an expanding range of clinical problems is the ability to conduct high-resolution imaging with a handheld scanner that ensures patient comfort and flexibility for the clinician. The scanner can be used to analyze various parts of the body without extra equipment or special operator training. Handheld MSOT scanners emit near-infrared light, usually in the range of 700–980 nm; they carry ultrasound detectors operating at central frequencies of 4–11 MHz; and they record data at video rates of up to 50 Hz (Karlas et al. 2017). These portable clinical systems achieve penetration depths of 2–5 cm (depending on the central frequency and tissue type) and spatial resolution better than 100 μm.

Building on our studies of BAT activation in mice, we succeeded in imaging supraclavicular BAT in humans previously shown to have BAT deposits by PET or MRI (Fig. 4a–c) (Reber et al. 2018). By illuminating the tissue at 28 NIR wavelengths from 700 to 970 nm in 10-nm steps, we were able to differentiate BAT from WAT based on their spectral characteristics (Fig. 4d). We were also able to detect BAT activation in response to cold exposure, which led to significant increases in oxy- and deoxyhemoglobin OA signal and therefore of TBV (Fig. 4e, f). These results suggest that MSOT has the capacity to track hemodynamic changes as a marker of BAT metabolic state, without the need for exogenous contrast agents. This may provide a unique opportunity for clinical application of MSOT, since it can provide rich, quantitative information about tissue physiology and function that is inaccessible to US, without requiring the extremely expensive infrastructure or radiation risks of other clinical imaging modalities such as MRI and PET.

Clinical Multispectral Optoacoustic Tomography Challenges and Perspectives for the Future

The time needed to acquire a full multispectral stack of images leaves today's handheld MSOT vulnerable to motion artifacts, which compromise spatial resolution and the accuracy of spectral unmixing. Such artifacts can be minimized as the clinician-operator becomes familiar with the setup and procedure. Other examples of motion artifacts which may threaten clinical MSOT imaging even when the scan head and patient remain still are the respiratory motion or the motion related to arterial pulsation. Recording data at higher frame rates or employing specialized motion correction algorithms usually suppress these and other types of motion artifacts (Taruttis et al. 2012). Another limitation of MSOT is that although it provides impressive imaging depth in the absence of exogenous contrast agents, the depth is currently insufficient for reliable localization and quantification of deeper BAT deposit such as the retroperitoneal.

It is likely that future improvements in illumination schemes, ultrasound sensors, and analysis methods will miniaturize scanning probes, improve image quality, and decrease post-acquisition processing times. This will enable large clinical studies to validate and exploit the potential of MSOT for imaging tissue physiology and
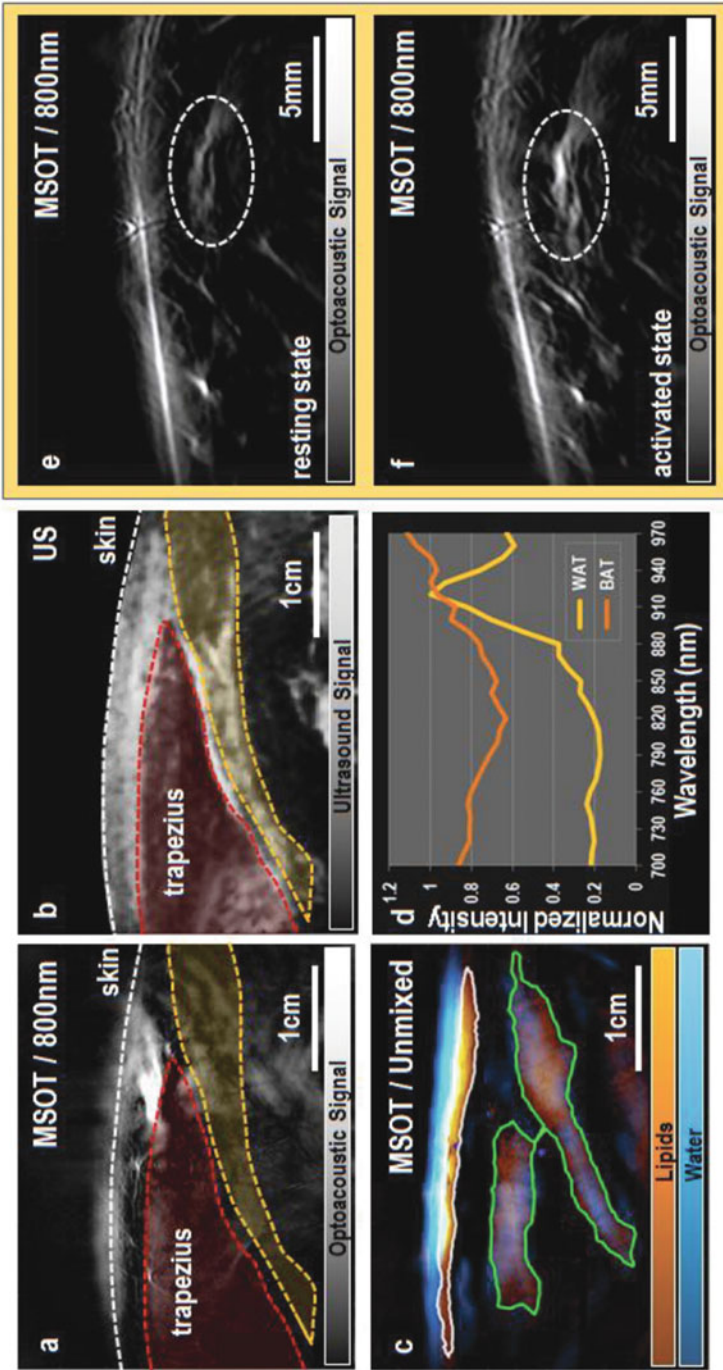
Fig. 4 In vivo imaging of supraclavicular BAT activation in humans using MSOT. Subjects were confirmed to have BAT deposits based on PET and MRI. (**a**) MSOT image (800 nm) showing the expected position of BAT (yellow region). The trapezius muscle is tinted in red. (**b**) US image corresponding to the field of view in panel (**a**). (**c**) MSOT image showing signal intensity attributed to lipid or water following spectral unmixing. Putative subcutaneous WAT is enclosed with a white line; putative trapezius muscle, with a green line on the left side of the image; and putative BAT, with a green line on the right side of the image. (**d**) Mean spectral profiles of the WAT and BAT regions delineated in panel (**c**). (**e**, **f**) MSOT images of supraclavicular BAT (**e**) in the resting state and (**f**) after 20 min of cold exposure to induce BAT activation. The region bounded inside the white dashed line shows an increased optoacoustic signal after BAT activation due to an increase in hemoglobin. Wavelength of 800 nm corresponds to the isosbestic point of HbO_2 and Hb in the NIR. Adapted with permission from Reber et al. (2018)

disease. In the case of BAT activation, further work should build on our findings so far (Reber et al. 2018) to establish the reproducibility of MSOT-based quantification and its correlation with the results of PET, MRI, and US. If MSOT can be validated, it can be applied in large trials to compare BAT mass and metabolic activity across patients with various metabolic disorders in the presence or absence of other comorbidities (e.g., cardiovascular).

References

Buehler A, Diot G, Volz T, Kohlmeyer J, Ntziachristos V (2017) Imaging of fatty tumors: appearance of subcutaneous lipomas in optoacoustic images. J Biophotonics 10:983–989

Cai X, Li L, Krumholz A, Guo Z, Erpelding TN, Zhang C, Zhang Y, Xia Y, Wang LV (2012) Multi-scale molecular photoacoustic tomography of gene expression. PLoS One 7:e43999

Cedikova M, Kripnerova M, Dvorakova J, Pitule P, Grundmanova M, Babuska V, Mullerova D, Kuncova J (2016) Mitochondria in white, brown, and beige adipocytes. Stem Cells Int 2016:6067349

Cypess AM, Weiner LS, Roberts-Toler C, Elía EF, Kessler SH, Kahn PA, English J, Chatman K, Trauger SA, Doria A, Kolodny GM (2015) Activation of human brown adipose tissue by a β3-adrenergic receptor agonist. Cell Metab 21:33–38

Dean-Ben XL, Gottschalk S, Mc Larney B, Shoham S, Razansky D (2017) Advanced optoacoustic methods for multiscale imaging of in vivo dynamics. Chem Soc Rev 46:2158–2198

Dima A, Ntziachristos V (2016) In-vivo handheld optoacoustic tomography of the human thyroid. Photoacoustics 4:65–69

Diot G, Dima A, Ntziachristos V (2015) Multispectral opto-acoustic tomography of exercised muscle oxygenation. Opt Lett 40:1496–1499

Diot G, Metz S, Noske A, Liapis E, Schroeder B, Ovsepian SV, Meier R, Rummeny E, Ntziachristos V (2017) Multispectral optoacoustic tomography (MSOT) of human breast cancer. Clin Cancer Res 23:6912–6922

Enerback S (2009) The origins of brown adipose tissue. N Engl J Med 360:2021–2023

Ernande L, Stanford KI, Thoonen R, Zhang H, Clerte M, Hirshman MF, Goodyear LJ, Bloch KD, Buys ES, Scherrer-Crosbie M (2016) Relationship of brown adipose tissue perfusion and function: a study through β2-adrenoreceptor stimulation. J Appl Physiol (1985) 120:825–832

Filonov GS, Krumholz A, Xia J, Yao J, Wang LV, Verkhusha VV (2012) Deep-tissue photo-acoustic tomography of a genetically encoded near-infrared fluorescent probe. Angew Chem Int Ed Engl 51:1448–1451

Giralt M, Villarroya F (2013) White, brown, beige/brite: different adipose cells for different functions? Endocrinology 154:2992–3000

Gottschalk S, Felix Fehm T, Luís Deán-Ben X, Razansky D (2015) Noninvasive real-time visualization of multiple cerebral hemodynamic parameters in whole mouse brains using five-dimensional optoacoustic tomography. J Cereb Blood Flow Metab 35:531–535

Gujrati V, Mishra A, Ntziachristos V (2017) Molecular imaging probes for multi-spectral opto-acoustic tomography. Chem Commun (Camb) 53:4653–4672

Herzog E, Taruttis A, Beziere N, Lutich AA, Razansky D, Ntziachristos V (2012) Optical imaging of cancer heterogeneity with multispectral optoacoustic tomography. Radiology 263:461–468

Jathoul AP, Laufer J, Ogunlade O, Treeby B, Cox B, Zhang E, Johnson P, Pizzey AR, Philip B, Marafioti T, Lythgoe MF, Pedley RB, Pule MA, Beard P (2015) Deep in vivo photoacoustic imaging of mammalian tissues using a tyrosinase-based genetic reporter. Nat Photonics 9:239–246

Jiang Y, Sigmund F, Reber J, Dean-Ben XL, Glasl S, Kneipp M, Estrada H, Razansky D, Ntziachristos V, Westmeyer GG (2015) Violacein as a genetically-controlled, enzymatically

amplified and photobleaching-resistant chromophore for optoacoustic bacterial imaging. Sci Rep 5:11048

Karlas A, Reber J, Diot G, Bozhko D, Anastasopoulou M, Ibrahim T, Schwaiger M, Hyafil F, Ntziachristos V (2017) Flow-mediated dilatation test using optoacoustic imaging: a proof-of-concept. Biomed Opt Express 8:3395–3403

Laufer J, Johnson P, Zhang E, Treeby B, Cox B, Pedley B, Beard P (2012) In vivo preclinical photoacoustic imaging of tumor vasculature development and therapy. J Biomed Opt 17:056016

Ntziachristos V (2010) Going deeper than microscopy: the optical imaging frontier in biology. Nat Methods 7:603–614

Ntziachristos V, Razansky D (2010) Molecular imaging by means of multispectral optoacoustic tomography (MSOT). Chem Rev 110:2783–2794

Omar M, Schwarz M, Soliman D, Symvoulidis P, Ntziachristos V (2015) Pushing the optical imaging limits of cancer with multi-frequency-band raster-scan optoacoustic mesoscopy (RSOM). Neoplasia 17:208–214

Philip R, Penzkofer A, Bäumler W, Szeimies RM, Abels C (1996) Absorption and fluorescence spectroscopic investigation of indocyanine green. J Photochem Photobiol A Chem 96:137–148

Razansky D, Vinegoni C, Ntziachristos V (2007) Multispectral photoacoustic imaging of fluorochromes in small animals. Opt Lett 32:2891–2893

Razansky D, Distel M, Vinegoni C, Ma R, Perrimon N, Köster RW, Ntziachristos V (2009) Multispectral opto-acoustic tomography of deep-seated fluorescent proteins in vivo. Nat Photonics 3:412–417

Reber J, Willershäuser M, Karlas A, Paul-Yuan K, Diot G, Franz D, Fromme T, Ovsepian SV, Bézière N, Dubikovskaya E, Karampinos DC, Holzapfel C, Hauner H, Klingenspor M, Ntziachristos V (2018) Non-invasive measurement of brown fat metabolism based on opto-acoustic imaging of hemoglobin gradients. Cell Metab 27:689–701.e684

Shu X, Royant A, Lin MZ, Aguilera TA, Lev-Ram V, Steinbach PA, Tsien RY (2009) Mammalian expression of infrared fluorescent proteins engineered from a bacterial phytochrome. Science (New York, NY) 324:804–807

Taruttis A, Claussen J, Razansky D, Ntziachristos V (2012) Motion clustering for deblurring multispectral optoacoustic tomography images of the mouse heart. J Biomed Opt 17:016009

Taruttis A, Timmermans AC, Wouters PC, Kacprowicz M, van Dam GM, Ntziachristos V (2016) Optoacoustic imaging of human vasculature: feasibility by using a handheld probe. Radiology 281:256–263

Tzoumas S, Ntziachristos V (2017) Spectral unmixing techniques for optoacoustic imaging of tissue pathophysiology. Philos Transact A Math Phys Eng Sci 375

Tzoumas S, Zaremba A, Klemm U, Nunes A, Schaefer K, Ntziachristos V (2014) Immune cell imaging using multi-spectral optoacoustic tomography. Opt Lett 39:3523–3526

Tzoumas S, Nunes A, Olefir I, Stangl S, Symvoulidis P, Glasl S, Bayer C, Multhoff G, Ntziachristos V (2016) Eigenspectra optoacoustic tomography achieves quantitative blood oxygenation imaging deep in tissues. Nat Commun 7:12121

Weber J, Beard PC, Bohndiek SE (2016) Contrast agents for molecular photoacoustic imaging. Nat Methods 13:639–650

Weissleder R (2001) A clearer vision for in vivo imaging. Nat Biotechnol 19:316–317

Weissleder R, Pittet MJ (2008) Imaging in the era of molecular oncology. Nature 452:580–589

Author Queries

Query Refs.	Details Required	Author's response
AU1	Please check if the presentation of the affiliations is fine.	
AU2	Please check if the presentation of the equal contribution footnote is fine.	
AU3	Keywords are required. Please provide the same.	
AU4	Please note that the reference style has been changed from Numbered to Name–Date style as per style.	
AU5	Please check if the section headings are assigned to appropriate levels.	